Low-frequency dynamic response and hysteresis in magnetic superlattices

S. Rakhmanova and D. L. Mills
Department of Physics and Astronomy, University of California, Irvine, California 92697

Eric E. Fullerton
Materials Science Division, Argonne National Laboratory, Argonne, Illinois 60439

(Received 28 April 1997; revised manuscript received 5 August 1997)

We study theoretically the low-frequency dynamic response of magnetic superlattices. We have the Fe/Cr(211) structure in mind, which has been demonstrated to have a surface or bulk spin-flop phase, depending on the number of magnetic layers. We proceed by integrating the equations of motion of the coupled magnetic films in time, for an extended period. We include Landau-Lifshitz damping in the equations of motion, and drive the structure with an appropriate low-frequency field. The externally applied (nominal) dc magnetic field is increased slowly. We can follow the structure through the sequence of magnetic-field-induced phase transitions. By this means, we obtain the magnetic phase diagram, χ_1 and χ_2, along with hysteresis curves in a single calculation. We also provide data on the magnetic-field dependence of the low-field susceptibility, which is in good accord with theory. [S0163-1829(97)07746-1]

I. INTRODUCTION

In recent years, magnetic multilayers of diverse character have been synthesized, and their properties studied extensively. In structures that incorporate films of ferromagnetic materials such as Fe, exchange couplings between adjacent Fe films are transmitted through the spacer layers between the Fe films. These are very weak compared to the strong effective exchange couplings between spins in a given Fe film. Thus, we may model the structure by representing each Fe film as a very large (and hence classical) spin **S**, formed from the spins within the film tightly linked by intra film exchange. The various classical spins then interact by the inter film exchange, and experience anisotropy or dipolar coupling relevant to any structure of interest.

Thus, magnetic multilayers such as those just described are a physical realization of one dimensional lines of classical spins. The inter film coupling is commonly antiferromagnetic in character, so in fact such systems are isomorphic to one-dimensional classical antiferromagnets. When placed in an external field, they then may exhibit a spin-flop phase, very much as found in crystalline antiferromagnets.[1]

Of particular interest as a model system are Fe/Cr(211) superlattices.[2] The Fe magnetizations lie within the plane parallel to the surface of the structure, and there is an easy axis within this plane, by virtue of the fact that the underlying unit cell is rectangular in shape. When the inter film exchange coupling is antiferromagnetic, the energy functional that describes the orientation of the moments is identical to that which applies to the (100) sheets of spins in the classical antiferromagnets FeF_2 and MnF_2. Thus, in zero external magnetic field, the ground state of the superlattice is antiferromagnetic, with sublattice magnetizations aligned along the easy axis in the plane. Application of a magnetic field parallel to the easy axis will induce a spin-flop phase, just as it does in MnF_2 and FeF_2 However, since the interfilm exchange couplings are very weak, such a phase may be studied with very modest magnetic fields.

Some years ago, it was noted that if the external field is applied antiparallel to the surface layer moments in an MnF_2 structure with a (100) surface, then at fields well below the bulk spin-flop field, the surface region ''flops'' first.[3] One thus has a surface spin-flop phase for magnetic fields below those that induce the bulk spin-flop transition. Recent experimental studies of the Fe/Cr (211) superlattices provide clear evidence for the presence of the surface spin-flop transition.[4] In a finite structure with an even number of layers, in the low-field antiferromagnetic state, necessarily one of the two surface films has its moment antiparallel to the applied field, a condition required for the surface spin-flop transition to occur.[3] If odd number of films is present, one realizes a ''bulk'' spin-flop transition, modified in character near the surface.

In an earlier paper,[4] theoretical studies were presented that trace the evolution of the superlattice from the low-field antiferromagnetic state, to the high-field ferromagnetic state, where the Fe film moments are all parallel to the field. For the case where the surface flop transition occurs, just above the critical field, the surface moment initially antiparallel to the external field rotates nearly 180°, to become almost parallel to it. In effect, a 180° twist has been applied to the antiferromagnet. A domain wall forms in the structure, initially located off center, in the direction of the ''flopped'' surface moment. Further increases in field cause the domain wall to move to the center of the superlattice, in a sequence of discrete hops. In effect, there is a magnetic analogue of the Peierls-Nabarro barrier experienced by a dislocation in a crystal lattice.[5] Each hop of the domain wall introduces a spike into dM/dH, as the domain wall moves to the center.[4] Further increases in field cause its width to increase, and a bulk spin-flop-like configuration is realized when the width of the wall becomes comparable to the size of the structure.

 © 1998 The American Physical Society

Very interesting subsequent work by Griffiths and his collaborators[6] shows a surface phase not discussed in earlier work[4] appears in a narrow field interval just above the surface spin-flop field.

The present paper is motivated by the appearance of the domain wall mentioned, which hops through the lattice very easily. The dynamic response of the structure should prove of great interest, in this field regime. Thus, we present theoretical studies of the low-frequency response of the superlattice structures, for the cases where an even or odd number of Fe layers is present and compare these calculations to ac susceptibility results of a 22-layer Fe/Cr(211) superlattice. We confine our attention to the regime where the response of the structure, as measured by the total ac moment induced by the external field, is linear. The theory accounts nicely for the principal features observed, though our model is not sufficient for us to obtain a full and complete account of the data.

In the linear response regime, we could describe the response of the structure within the framework of spin-wave theory, where the externally applied ac field couples to the collective spin-wave modes of the superlattice. The theory of the collective spin-wave modes has been developed and described earlier, with attention to the surface spin-flop regime.[7] These modes have been studied experimentally by Brillouin light scattering, and the key features of the Brillouin spectrum are reproduced in theoretical calculations.[8]

Instead, we introduce here an approach that, in a single numerical study, provides us with a remarkably complete description of the response of the structure both to the externally applied static field H_0, and the ac field $h \sin \Omega t$.

We proceed as follows. We begin by placing the system in a weak external field H_0, so it resides in its antiferromagnetic ground state. The ac field is turned on, and we integrate the equations of motion of the spin system forward in time. We add damping for each spin, of the Landau-Lifshitz form $-\gamma(\mathbf{S}_i \times \dot{\mathbf{S}}_i)$.

In the presence of this damping, the transients die down, and the spins settle into steady state motion. We may calculate the total transverse moment as a function of time, and Fourier transform this to obtain the real and imaginary part of the low-frequency ac susceptibility, $\chi_1(\Omega)$ and $\chi_2(\Omega)$.

We then increase the dc field H_0 very slowly; in this manner we obtain χ_1 and χ_2 as functions of H_0. When we cross the spin-flop fields, the structure relaxes into its lowest energy state, by virtue of the damping present. Thus, the system spontaneously ''flops,'' and by monitoring the total transverse moment we obtain χ_1 and χ_2 in the spin-flop phase. At the same time this is done, we may calculate the magnetic moment parallel to the (nominally) dc field H_0. We thus obtain the dc magnetization, as a function of H_0 at the same time. The magnetization curves we obtain in this manner are in excellent agreement with those calculated earlier,[4] by minimizing the energy of a static spin array for each value of H_0.

The surface and bulk spin-flop transitions are first order, and thus display hysteresis. By first increasing H_0 until we reach the high-field saturated ferromagnetic state, then decreasing this field until it changes sign, we may also generate hysteresis curves for the structure.

We thus obtain a large amount of information with this method, in a relatively straightforward manner, within a framework of a single calculation. While we could use spin-wave theory to generate expressions for $\chi_1(\Omega)$ and $\chi_2(\Omega)$, as remarked above, the algebraic analysis required would be quite involved, for the complex magnetic phases of the finite structure. The equation of motion method is both conceptually simple and elegant and, as we demonstrate here, works remarkably well.

Our decision to approach this problem by this method was influenced by an interesting paper on domain walls in antiferromagnets published by Papanicolaou.[9] Rather than generate a description of domain walls by minimizing the energy of an antiferromagnet to which a 180° twist is applied at one end, Papanicolaou began at time $t=0$ with the spins arranged to mimic a domain wall in an approximate and crude manner. He then numerically integrated the equations of motion of the damped spin system forward in time, to find the spins relaxed into their lowest energy state at long times. With the constraint that one end spin is twisted 180°, he obtained impressively accurate descriptions of domain walls, noting in the process that these walls posses a ferromagnetic moment parallel to the easy axis. Here we show that by applying an ac field, and varying the dc field slowly in time as described above, the equation of motion method may be used to obtain the magnetic phase diagram, hysteresis loops, along with $\chi_1(\Omega)$ and $\chi_2(\Omega)$ in a single calculation.

II. THE MODEL AND THE METHOD OF CALCULATION

We consider a superlattice which consists of N ferromagnetic films, and $\mathbf{M}_i$ is the magnetization of the ith film. The $\hat{y}$ axis will be chosen perpendicular to the interfaces between films, and the $\hat{z}$ axis, in the plane parallel to the interfaces, is the easy axis. An external dc field H_0 is applied parallel to the easy axis. We then describe the system by an effective Hamiltonian

$$\hat{H} = A \sum \mathbf{M}(i) \cdot \mathbf{M}(i+1) - H_0 \sum M_z(i) - K \sum M_z^2(i) + 2\pi \sum M_y^2(i) - h \sin\Omega t \sum M_x(i). \quad (1)$$

Here K is an anisotropy constant which renders the z axis an easy axis, and the term in $M_y^2(i)$ is the shape anisotropy with origin in the dipolar field generated by tipping the magnetization out of the xz plane. While this term plays no role in the energetics of the various magnetic ground states realized in the external field H_0, it enters the description of the dynamical response of the structure, since the spins precess in an elliptical manner, tipping out of the plane as they do. We assume $A>0$, so we have antiferromagnetic coupling between adjacent films. The last term is the weak externally applied ac field discussed in Sec. I.

The equations of motion we study can be written in the form

$$\frac{\partial \mathbf{M}(i)}{\partial t} = [\mathbf{M}(i) \times \mathbf{H}_{\text{eff}}(i)] - \gamma[\mathbf{M}(i) \times \dot{\mathbf{M}}(i)], \quad (2)$$

where the effective field $\mathbf{H}_{\text{eff}}$ acting on the ith moment is

$$\mathbf{H}_{\rm eff}(i)=[H_0+2KM_z(i)]\hat{z}-2A[\mathbf{M}(i+1)+\mathbf{M}(i-1)] -4\pi M_y(i)\hat{y}+\hat{x}h\ \sin\Omega t. \tag{3}$$

We have added damping of the Landau-Lifshitz form to the right hand of Eq. (2). From the point of view of the questions we wish to explore here, the virtue of damping of this form is that $\mathbf{M}(i)$ relaxes without changing its length.

We rewrite Eq. (2) in terms of the unit vector

$$\hat{n}(i)=\frac{\mathbf{M}(i)}{M_s}, \tag{4}$$

where M_s is the saturation magnetization of the film. Then we introduce the effective anisotropy field

$$H_A=2KM_s \tag{5}$$

and the exchange field

$$H_E=2AM_s, \tag{6}$$

to write

$$\frac{\partial\hat{n}(i)}{\partial t}=[\hat{n}(i)\times\mathbf{H}_{\rm eff}(i)]-g[\hat{n}(i)\times\dot{\hat{n}}(i)], \tag{7}$$

where now

$$\mathbf{H}_{\rm eff}(i)=[H_0+H_A\hat{n}_z(i)]\hat{z}-\frac{H_E}{2}[\hat{n}(i+1)+\hat{n}(i-1)] -4\pi M_s\hat{n}_y(i)+\hat{x}h\ \sin\Omega t \tag{8}$$

and $g=\gamma M_s$. Of course, it is essential to realize the films at each end of the superlattice are exchange coupled to only one neighbor in the film interior.

We next turn to a discussion of the procedure we have used to integrate the equations of motion. First of all, we write $\hat{n}(i)$ in spherical coordinates:

$$\hat{n}(i)=(\sin\theta_i\ \sin\phi_i,\cos\theta_i,\sin\theta_i\ \cos\phi_i), \tag{9}$$

with the angle θ_i measured from the $\hat{y}$ axis. We apply free end boundary conditions, wherein each end film is exchange coupled to only one interior neighbor. Upon substitution of Eq. (9) into Eq. (6), we may reduce the problem to the solution of $2N$ equations, where N is the number of Fe films in the superlattice. To facilitate comparison with calculations reported in Refs. 4 and 7, most of the results reported here are for $N=15$ and $N=16$. We have performed calculations for N in the range of a few hundred, it should be remarked, to obtain accurate results very quickly.

We scale the various quantities that enter by measuring them in units of kilogauss. We shall choose $4\pi M_s/H_E=21$, and $H_A/H_E=0.125$. The ratio of H_A/H_E just given is appropriate for the Fe/Cr(211) structure, and we choose $H_E=2$ kG. We take $4\pi M_s$ to be 21 kG, appropriate to bulk Fe. We remark that is not the purpose of this paper to provide a full quantitative account of the data on the samples discussed here and in Ref. 4. To do so would require elaboration of the basic model, with inclusion of biquadratic exchange that is surely present. The parameters just stated provide us with transition fields rather close to those observed. The unit of time will be $\tau=(H_E/2)t$; one divides the equations of motion by $H_E/2$, and rescales the time in this manner. These numbers are somewhat different than those employed in Refs. 4 and 7. We have reduced the strength of the anisotropy field, to bring the value of the surface spin-flop field closer to those in the sample studied here.

To proceed, we exploit the fact that the ground state of the system for zero external dc field H_0 is known exactly. This is the simple antiferromagnetic state of Néel character, which corresponds to choosing all $\theta_i=\pi/2$, and ϕ_i to be 0 for odd i, and π for even i. We use this condition as an initial configuration. We then increase the external field linearly with time, integrating the equations of motion continuously as we do so. The slope $d(H_0/H_E)/d\tau$ is chosen to be 10^{-4}. We select $(g/H_E)=0.1$, so that in a dimensionless time interval $\Delta\tau\cong10$, the system relaxes in response to any change. In the time interval $\Delta\tau\cong10$, (H_0/H_E) changes by only one part in 10^3. The system thus adiabatically follows changes in the dc field. The ac field (discussed further below) weakly excites the system, so as soon as the energy of a spin-flop state drops below that of the low-field antiferromagnetic state, as H_0 increases, the system is stimulated to make a transition into the new low-energy spin-flop state. The Landau-Lifshitz damping allows the spins to lose energy through dissipation into the reservoir responsible for the damping, so to speak. To integrate the equations of motion, we use the DDEBDF code from the package of differential equation solvers DEPAC that was developed at the Lawrence Livermore Laboratory. The code uses the backward differentiation formulas to solve first-order stiff differential equations. It advances the solution using step sizes that are automatically selected so as to achieve the desired accuracy. Ordinarily, a time step is of order 1, except in the vicinity of a phase-transition point where it becomes the order of 10^{-1}. To sweep out a typical magnetization curve such as those shown below requires integrating the equations of motion for a dimensionless time interval in the range of 5×10^4. This requires about five minutes on a DEC Alpha workstation. If in addition, one obtains $\chi_1(\Omega)$ and $\chi_2(\Omega)$, perhaps a half hour of computer time is required.

It is useful, for the purpose of obtaining a physical feeling for the time scales discussed above, to examine the collective spin-wave frequencies of the superlattice structure. For the finite superlattice modeled as we do here, one finds detailed calculations in Ref. 7. For a structure of infinite length, one may work out the dispersion relation from the equations of motion given above. We have done this to find a two branch dispersion relation in the low-field antiferromagnetic state. If we consider a spin wave that propagates in the $\hat{y}$ direction with wave vector q, we find

$$\Omega_{\pm}^2(q)=\Omega_0^2(q)+H_0^2+4\pi M_s(H_A+H_E)\pm2[H_0^2\Omega_0^2(q) +4\pi H_0^2M_s(H_A+H_E+\pi M_s) +4\pi^2M_s^2H_E^2\cos^2(q/2)]^{1/2}, \tag{10}$$

where

$$\Omega_0(q)=[(H_A+H_E)^2-H_E^2\cos^2(q/2)]. \tag{11}$$

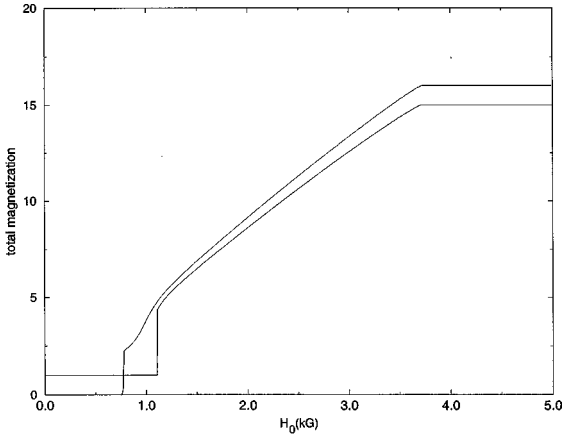

FIG. 1. The component of magnetization, parallel to the dc field H_0, as a function of H_0 for a sample with 15 Fe layers, and a sample with 16 Fe layers. H_0 is dimensionless and is measured in units of H_E.

In an antiferromagnetic resonance experiment, one excites the $q=0$ modes. In zero external magnetic field we have for the two modes

$$\Omega_+^2(0)=(H_A+4\pi M_s)(H_A+2H_E), \tag{12a}$$

$$\Omega_-^2(0)=H_A(H_A+4\pi M_s)+2H_AH_E. \tag{12b}$$

The parameters above give $\Omega_+(0)=9.5$, and $\Omega_-(0)=2.51$, in units of kilogauss.

In dimensionless form, the ac field is written $(h/H_E)\sin(\omega\tau)$, where for most of the calculations below, we choose $\omega=0.1$. In this paper, we are thus exploring the response to frequencies well below the spin-wave frequencies just discussed. We have chosen $(h/H_E)=10^{-4}$ in all results shown below. The period of the driving field is $\Delta\tau=20\pi=62.8$ time units. This is very long compared to the time $\Delta\tau=10$ for transients to die out in the system, but still so short that dc field changes very little over one cycle of oscillation. When we calculate $\chi_1(\Omega)$ and $\chi_2(\Omega)$, we need to have the dc field constant over many cycles of oscillation of the ac field. For this purpose, we thus increase it in a stepwise fashion, rather than the linear manner discussed above. Each step in the field is taken to be 150 periods of the ac field. We use data from the last 10 periods in this sequence to fit the total transverse moment to the form $\chi_1\sin(\omega\tau)+\chi_2\cos(\omega\tau)$ by a χ-squared procedure. We have also Fourier transformed the transverse moment, to confirm only a single frequency is present in the output, for the range of (h/H_E) employed.

We now turn to our results.

III. RESULTS AND DISCUSSION

In Fig. 1, for the case where the superlattice has 15 Fe films, and also 16 Fe films, we show the z component of magnetization M_z as a function of the dc magnetic field H_0. If these are compared to the magnetization curves calculated by minimizing the static energy of the Hamiltonian in Eq. (1) (with $h=0$), one sees excellent agreement, save for the fact that the spin-flop fields are somewhat lower, because of our use of a smaller anisotropy field. One further point is discussed below. For the case $N=15$, we realize a ''bulk'' spin flop, of course modified by the presence of the two surfaces. The discontinuity in M_z just above $H_0=1.0$ is the signature of the spin-flop transition. So far as we can tell, the transition occurs right at the field where the static energy of the flopped state drops below that of the low-field antiferromagnetic state.

For the case $N=16$, we realize the surface spin-flop transition, which occurs for a value of H_0 reduced from that for the case $N=15$ by roughly a factor of $\sqrt{2}$, as expected[3] when $H_A \ll H_E$.

We turn to one difference between the present results, and those reported earlier[4] for the case $N=16$. The static calculations showed that as H_0 is increased above the surface spin-flop field, the surface moment rotates by nearly 180°, to become nearly parallel, rather than antiparallel to the external field. It is as if the antiferromagnet has one end spin twisted by nearly 180°. There is then a domain wall in the structure, between two nearly antiferromagnetic regions. As H_0 is increased, the domain wall executes discontinuous jumps, as it migrates to the center of the structure, to ultimately widen and evolve into a bulk spin-flop-like state. It should be remarked that the energy differences between the states with the domain wall in different locations were very small indeed. While, as we discuss below, we see the domain wall form in the present calculations and migrate toward the center of the structure with increasing field, it does so smoothly so far as we can discern by eye. It may be difficult to perceive the jumps, or possibly in the presence of the ac field, the wall moves smoothly through the structure.

In Fig. 2, we illustrate how the system evolves from the low-field antiferromagnetic state, to the high-field saturated ferromagnet, for $N=15$ and for $N=16$. We can see clearly that when $N=15$, the entire structure ''flops'' at once. The spins at the two ends of the structure are pulled closer to the dc field than those at the center, because they are exchange coupled to only one neighbor, rather than two, as is the case for the interior spins.

For $N=16$, we illustrate the surface spin flop, with formation of the domain wall and its subsequent migration to the center. Once it is centered, its width increases continuously, and the system evolves into a bulk spin-flop-like state.

There is one interesting aspect to the sequence of events illustrated in Fig. 2, for the case $N=16$. If one looks at the pattern of arrows in the low-field antiferromagnetic state, the picture is odd under reflection through its midpoint. The final ferromagnetic state is even. There is a field at which the domain wall is centered precisely in the film center, and at this point the ''pattern of arrows'' is even under reflection for all higher fields. We thus have a mechanism for evolution from the odd- to the even-parity state. For $N=15$, the pattern of arrows is even under reflection through the midpoint of the structure at all fields.

In Figs. 3 and 4, we show the evolution of the surface spin-flop state with increasing magnetic field, in a very narrow interval of field just above the surface spin-flop field. We have a sequence of ''snapshots''; the dc field changes by about 0.2% in magnitude from the beginning to the end of the sequence. In essence, the domain wall continuously creeps into the structure from right to left, as the dc field increases. In the first illustration in Fig. 3, there is a very

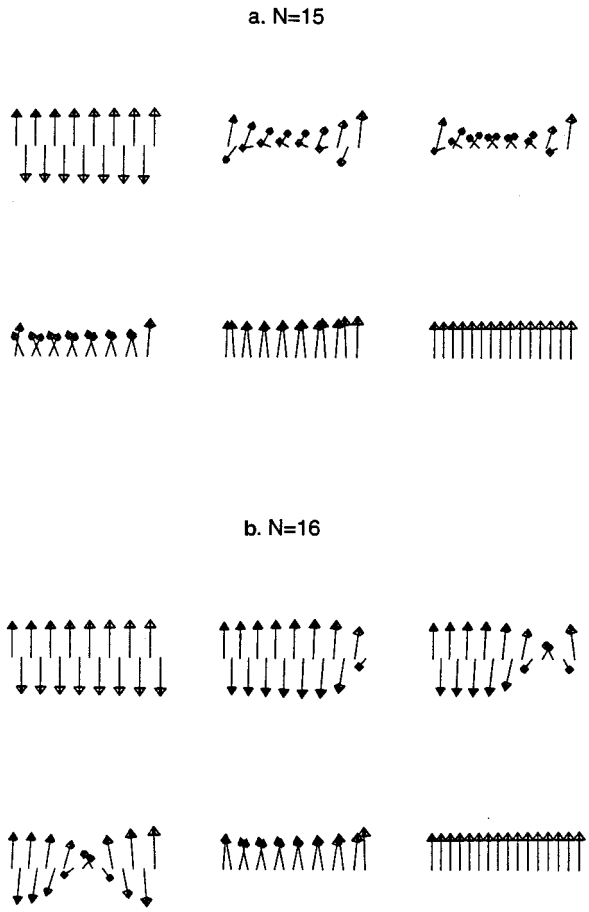

FIG. 2. Moment configurations as the strength of the dc field is increased, for (a) the case where there are 15 Fe films, and (b) the case where there are 16 Fe films. These are not strict side views of the structure, but the backbone of the structure is canted out of the page a bit, to provide perspective.

slight tipping of the unstable spin; the tail of the domain wall has crept in a bit at this point. The system evolves very quickly, over a narrow field interval, to a state where the unstable moment is twisted nearly 180°. We believe that in each of the panels in Figs. 3 and 4, we have a fully relaxed moment configuration. We see no clear evidence of the ''true surface spin-flop state'' discussed in Ref. 6, unfortunately. The surface spin does seem to ''hang up'' a bit when it makes an angle of roughly 60° with the external field, as expected for their state, but we cannot identify a clear signal of this phase.

By sweeping the field first upward, until we reach the saturated ferromagnetic state, and then decreasing the field back downward past the spin-flop transition, we can generate hysteresis curves. The magnetization exhibits irreversible behavior only in the near vicinity of the spin-flop transition.

In Fig. 5(a), for $N=15$, we show hysteresis curves calculated by ramping the field up linearly in time, and then ramping it back downward linearly in time, until the field changes sign and we reach the saturated ferromagnetic state with all moments pointing downward. Fig. 1, as we have discussed, gives the total magnetization as a function of field, when one starts at zero field and ramps it up to the saturated ferromagnetic state. The dashed line in Fig. 5(a) give the magnetiza-

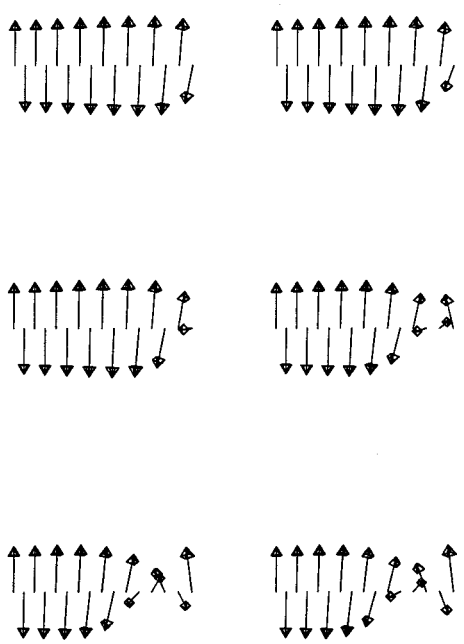

FIG. 3. Selected ''snapshots'' of the spin lattice, for a narrow interval of time in the near vicinity of the surface spin-flop transition. Again we have $N=16$. From the beginning to the end of the sequence, the dc magnetic field changes by 0.2%. The view is side view, but with the axis canted out of the plane a bit, to assist in viewing the spin array. Each spin configuration shown is a stable, relaxed configuration.

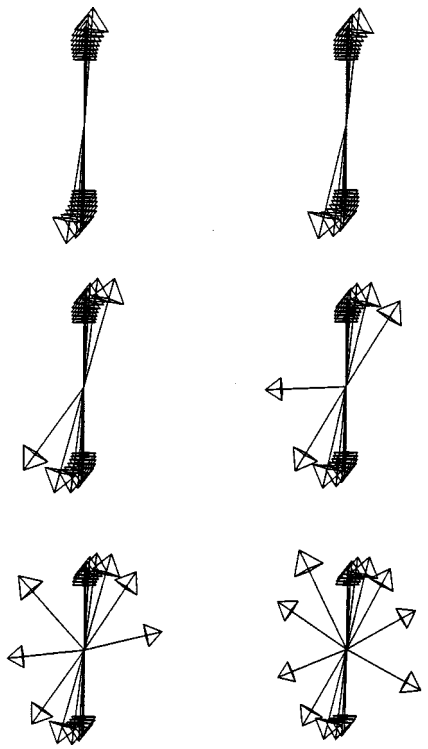

FIG. 4. An end on view of the spin array for the same fields used in Fig. 3.

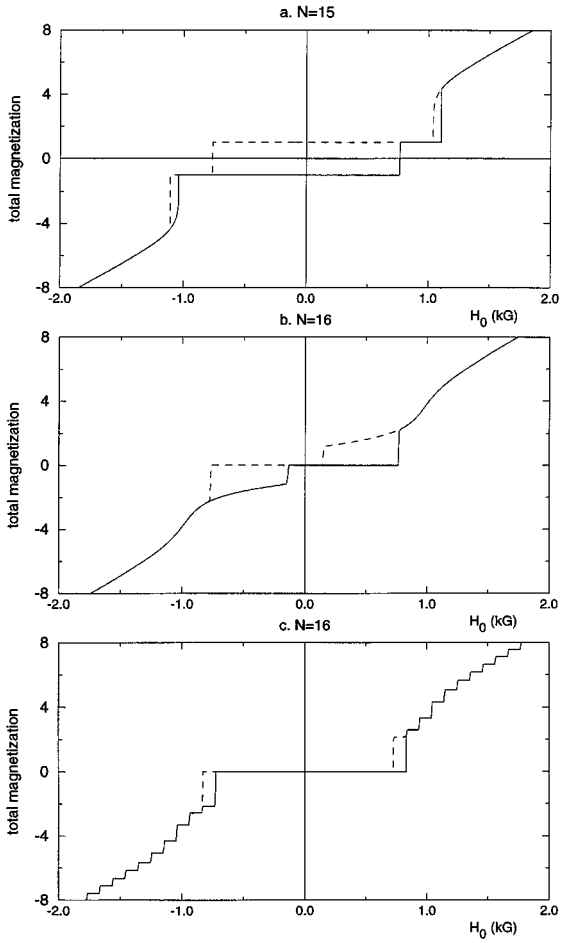

FIG. 5. Hysteresis curves, for (a) the case $N=15$, and (b) the case $N=16$, for the case where the dc magnetic field is ramped up or down linearly with time. In (c), we show a curve when the field is increased in small steps. Strictly speaking, the horizontal axis should be labeled with time rather than field, but the steps in field are small. In Fig. 1, we show the magnetization when one begins in zero field, and increase the field to achieve the saturated ferromagnetic state. In these figures, dashed curves describe the magnetization as one decreases the field from a large positive value, to a large negative value, while the solid curve describes the magnetization when one starts from large negative field, and increases the field.

tion as a function of field, as one comes down in field. Then once the saturated state is reached for strong negative fields, the solid line is the magnetization as one ramps the field back up. It is striking that the coercive field for $N=15$, defined as the field where the net magnetization rotates to align with the field after its sign reverses, agrees very accurately with the value of the surface spin-flop field for the case $N=16$.

In Fig. 5(b), we show the hysteresis curves calculated for the case $N=16$. Notice that the amount of hysteresis is very much larger than for $N=15$. We believe this is because, at high fields, the system is in the symmetric state described above. It is difficult for the spins to make the transition back to the low-field asymmetric state. They remain ''locked'' in the symmetric state until very low fields.

Hysteresis curves were also calculated earlier in the paper by Wang and Mills,[7] by searching for the limits of stability of various states, through minimizing their static energy,

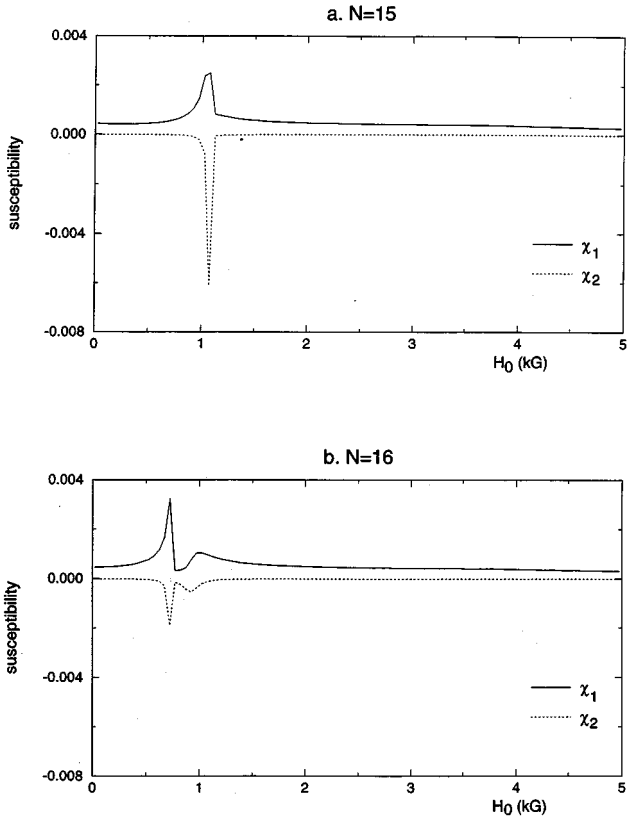

FIG. 6. Calculations of χ_1 and χ_2 as a function of field, as one begins in zero external field, and increases it to reach the saturated ferromagnetic state. Again we show results for (a) the case $N=15$, and (b) the case $N=16$.

then testing for stability. The results are remarkably similar to those in Figs. 5(a) and 5(b), except the equivalent of the dashed line in Fig. 5(b) extended down to zero dc field. We believe the small difference has its origin in the presence of the ac field in our simulation, which can stimulate the transition. Also, if the time profile of the dc field is decreased in a steplike manner, as one comes down in field, the transition to the asymmetric state occurs much sooner for the case where the system receives a sequence of impulsive ''blows'' through the sudden change in the dc field. We illustrate this in Fig. 5(c).

Now we turn our attention to calculations of the dynamic susceptibilities $\chi_1(\Omega)$ and $\chi_2(\Omega)$. We change the dc field in steps, as mentioned earlier. After a given step, when the transients die down, we fit the total transverse moment to the expression

$$m_T(t)=h[\chi_1(\Omega)\sin(\Omega t)+\chi_2(\Omega)\cos(\Omega t)], \qquad (13)$$

where in the convention of Eq. (13), in fact $\chi_2(\Omega)$ is negative.

In Fig. 6, we show χ_1 and χ_2 as a function of field, with χ_1 given as a solid line and χ_2 as a dashed line. The calculations assume one begins in zero field, and increases the field until the saturated ferromagnetic state is reached. For $N=15$, we see a clear signature at the spin-flop transition, while for $N=16$, we see a feature at the surface spin-flop transition and a second bump located near the bulk spin-flop

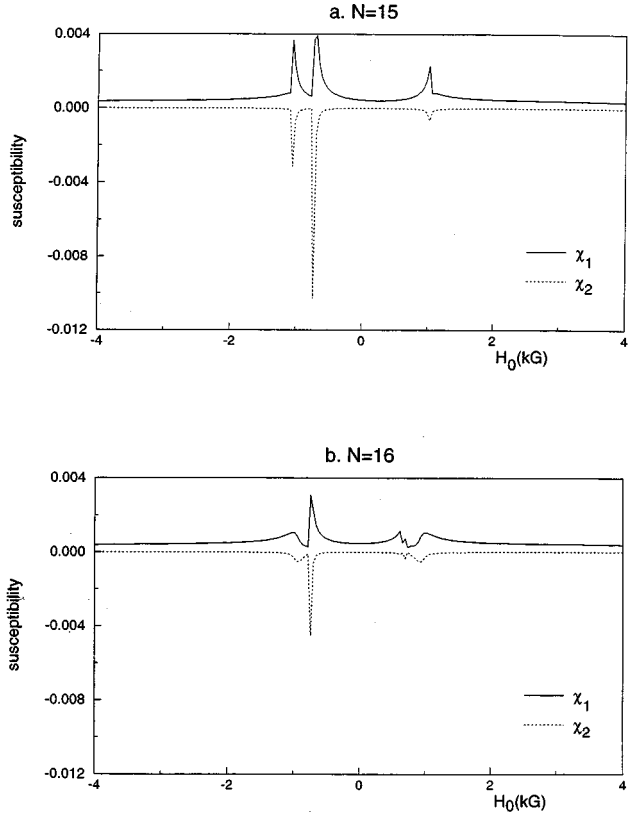

FIG. 7. The same as Fig. 6, but now we begin in the saturated ferromagnetic state, and decrease the field to reach large negative fields.

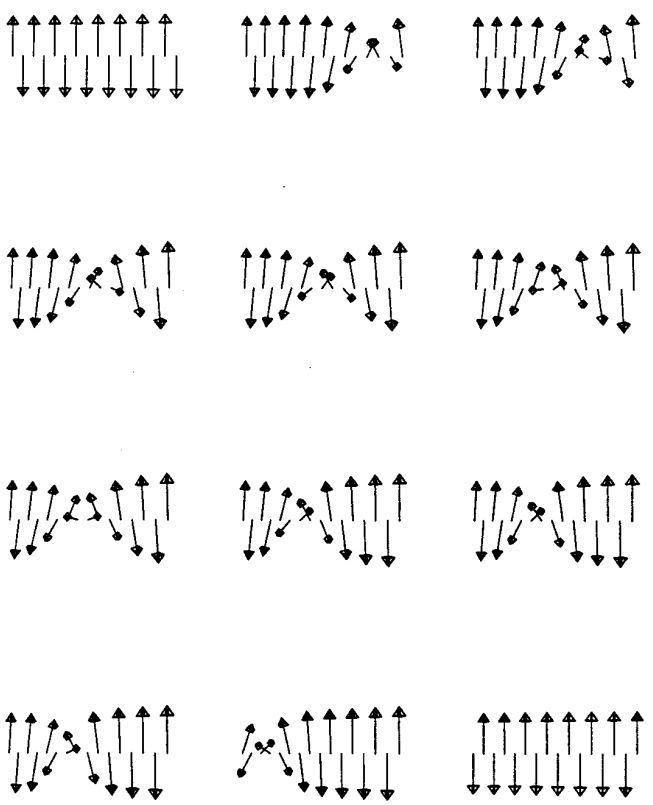

FIG. 8. For $N=16$, we show a series of snapshots of the field excursions that interchange the two degenerate antiferromagnetic ground states.

field. As the number of spins N increases, the feature at the surface spin-flop transition becomes smaller, and the bump at the bulk spin-flop grows and sharpens.

In Fig. 7, we show calculations in which the system is initially saturated in the high-field state, and the field is then decreased until we reach the saturated state at large negative fields. For the case $N=15$, we see a two peaked structure at negative fields. That at lowest (negative field) is associated with the coercive field of the structure where its total moment reverses, and the second with the subsequent bulk spin-flop transition. For $N=16$, we see a very large asymmetry, between the structures at positive and negative fields.

We have found very striking behavior of the structure, upon traversing the hysteresis loop in Fig. 5(b) appropriately. We begin with the antiferromagnetic state in zero field which we might call the AB state. By this we mean that the leftmost moment, designated by A, points upward, while the rightmost moment, designated by B, is directed downward. Note this state is degenerate in energy with configuration BA. Once again, we begin in zero field, and increase the dc field past the surface spin-flop field to, say, the knee in the reversible part of the M-H diagram in Fig. 5(b). Then we decrease the field back to zero.

The behavior of the structure is illustrated in the series of panels displayed in Fig. 8. We see the initial AB state, and the domain wall that enters the structure from the right, and progresses to the center of the structure. As the field is decreased in this state, the wall keeps moving from right to left, to exit the structure from its left side, so to speak. We are left with the BA structure in the final state. This operation has interchanged the two degenerate antiferromagnetic ground states.

As remarked briefly in Sec. I, we have measured the ac susceptibility, to obtain values of χ_1 and χ_2 as a function of field, on the Fe/Cr(211) superlattice described in Ref. 4, which exhibited the surface spin-flop transition. The ac susceptibility and dc magnetization were measured in a Quantum Design PPMS 6000 with a 14 G, 1000 Hz ac field was parallel to the dc applied field. Thus, when comparing theory and experiment, one must recognize that in the experiment, the ac field is parallel to the dc field, while the calculations generate the transverse response. This difference clearly deserves comment. In our theoretical studies of the phase diagram and hysteresis curves, application of a time varying field would not stimulate spin reorientation transition, when one approached the transition field from either the low-field antiferromagnetic state, or the high-field ferromagnetic state, since such a field exerts no torque on the spins. Thus, we have used a transverse field in our theoretical studies. In the data on χ_1 and χ_2, the signal is only large in the spin-flop region. We expect a rather small difference between the dynamic susceptibilities calculated for longitudinal or transverse fields in this state, so we believe it appropriate to compare the theory and the experimental data, for semiquantitative purposes. In Fig. 9(a) we show the dc magnetization as a function of dc field. The surface spin-flop transition occurs at $\approx$1000 G in this sample. There is clear

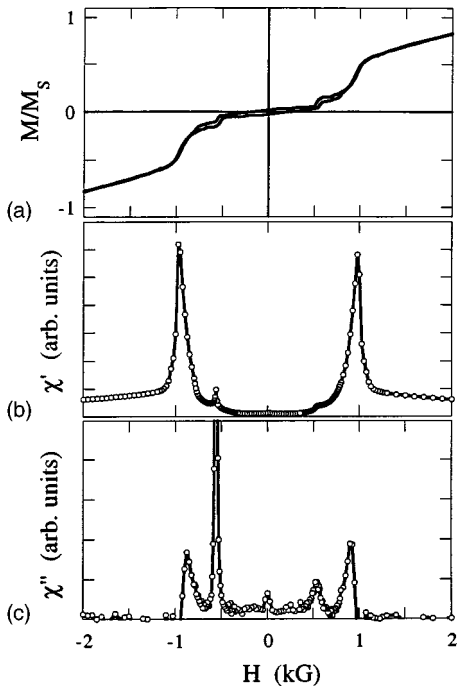

FIG. 9. Experimental measurements for (a) total magnetization of the sample described in the text as a function of dc field, (b) χ_1 and (c) χ_2 the real and imaginary parts of susceptibility, respectively.

hysteresis in the near vicinity of the surface spin-flop transition, though one sees less hysteresis than is evident in our simulations. The experimental results more closely resemble the simulation in Fig. 5(c) where the applied field is changed in steps.

Figure 9(b) shows χ_1, the real part of the susceptibility, taken on a field sweep that begins in the saturated ferromagnetic state ($H>3$ kG), with H along $+\hat{z}$ to saturation along $-\hat{z}$. We see features near ± 1000 G, the bulk spin-flop state of an infinitely long structure in agreement with previous static susceptibility (dM/dH) results of Ref. 4. We only see very modest signature of the surface spin-flop transition that was prominent in the static susceptibility. We believe that the reason for the absence of structure in χ_1 at the surface spin flop results from the hysteresis near this transition. A minor loop about the surface spin-flop transition determined a coercive field of ≈ 30 G that is large compared to the ac driving field. Therefore, in these measurements, the ac field is not sufficient to sample reversibly the surface spin-flop transition.

Shown in Fig. 9(c) is the imaginary part χ_2 of the sweep in Fig. 9(b). We again see features at the bulk spin flop that have roughly equal strength at positive and negative fields and are enhanced to the low-field side of the transition. Above the bulk spin flop the value of χ_2 is below the sensitivity of our magnetometer. Surprisingly, there is also structure at the surface spin-flop transition that is highly asymmetric. We find that the dramatic peak in χ_2 at the spin-flop transition when the applied field is swept from $H=0$ toward saturation is missing.

We have carried out simulations for the 22-layer film, employing values of H_A and H_E used in the calculations discussed earlier. It should be noted that we cannot employ

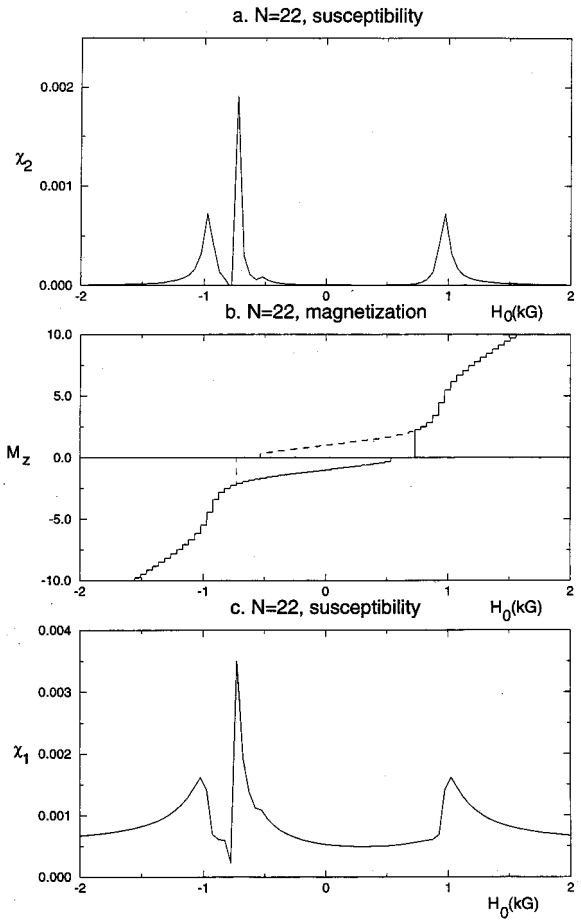

FIG. 10. Calculations for (a) χ_2, and (c) χ_1 as a function of field for 22-layer structure. In (b), we show the corresponding hysteresis curve. Here H_0 is given in kilogauss.

frequencies as low as those used in the experiments, since the integration times would be prohibitively long. In the samples used, the spin-wave frequencies are in the range of a few tens of GHz.[8] Thus, if Ω_{SW} is a typical spin-wave frequency, in the experimental measurement, $\Omega/\Omega_{\mathrm{SW}} \approx 3 \times 10^{-8}$. In our simulations, from the spin-wave frequencies quoted in Sec. II, $\Omega/\Omega_{\mathrm{SW}} \approx 5 \times 10^{-2}$. However, so long as the ac frequency is very small compared to the spin-wave frequencies, we are in the regime where the spins follow the ac field nearly adiabatically, with a phase lag provided by the finite value of $\Omega\tau$. In this low-frequency regime, where the ac field has simple relaxational form, the field dependence realized is not sensitive to frequency. In the simulations reported here, the ac driving field is also smaller than that used in the experiments, by a bit more than a factor of 10. We have carried out calculations for ac driving fields in the range used in the experiments (indeed we have explored even larger fields), to find results for χ_1 and χ_2 identical to those reported.

Nonetheless the simulations reproduce the key features of the data very nicely. We show the field dependence of χ_2 in Fig. 10(a), as the field is decreased from high positive values, to large negative values. We see the two symmetric structures at the bulk spin-flop field, and the very large, dramatic spike at $-H_{\mathrm{SSF}}$, with H_{SSF} the surface spin-flop field. We do

not see the small structure evident in the data at $+H_{SSF}$. The reason for this is the very different hysteresis curve found in the simulations. As we lower the field, the 22-layer model structure remains locked in the symmetric state until rather large negative fields are reached. We show our calculated hysteresis curve in Fig. 10(b), for this model structure. The coercive field at which the system returns to the antiferromagnetic ground state is negative; note the small jump in M_z just before one reaches $-H_{SSF}$. One sees a small structure in χ_2 at this field, in Fig. 10(a).

Save for the difference between the theoretical and experimental coercive fields, we thus obtain an excellent account of the χ_2 data in our simulations. In Fig. 10(c), we show χ_1 as a function of field. We again see symmetric structures at the bulk spin-flop field (very similar to those in the data), but now we see a major feature at $-H_{SSF}$ as well. We expect this structure should be present in the data as well, if the experiments could be carried out in a transverse ac field.

IV. CONCLUDING REMARKS

The method of calculation employed here allows one to generate magnetic phase diagrams, hysteresis curves, and accounts of the dynamic response of one-dimensional classical arrays of spins, in one single computation. While the results reported here explore a relatively small number of spins, since we wish to compare our new results with data and the earlier theoretical literature, we emphasize that we have applied the technique to several hundred spins with no difficulty. Thus, the direct integration of the equations of motion should prove a most useful technique for studies of a wide range of magnetic nanostructures.

ACKNOWLEDGMENTS

The research at Irvine was completed with support from the Army Research Office, under Contract No. CS0001028, and that at Argonne National Laboratory by the U.S. Department of Energy, BES-Materials Science, under Contract No. W-31-109-ENG-38.

[1] S. Foner, in *Magnetism*, edited by G. Rado and H. Suhl (Academic, New York, 1993), Vol. 1, Chap. 9, p. 338.
[2] Eric E. Fullerton, M. J. Conover, J. E. Mattson, C. H. Sowers, and S. D. Bader, Phys. Rev. B **48**, 15 755 (1993).
[3] D. L. Mills, Phys. Rev. Lett. **20**, 18 (1968); F. Keffer and H. Chow, *ibid.* **31**, 1061 (1973).
[4] R. W. Wang, D. L. Mills, Eric E. Fullerton, J. E. Mattson, and S. D. Bader, Phys. Rev. Lett. **72**, 920 (1994).
[5] J. Friedel, *Dislocations* (Pergamon, Oxford, 1964), p. 54.
[6] C. Micheletti, R. B. Griffiths, and J. M. Yeomans, J. Phys. A **30**, L233 (1997).
[7] R. W. Wang and D. L. Mills, Phys. Rev. B **50**, 3931 (1994).
[8] R. W. Wang, D. L. Mills, Eric E. Fullerton, Sudha Kumar, and M. Grimsditch, Phys. Rev. B **53**, 2627 (1996).
[9] N. Papanicolaou, Phys. Rev. B **51**, 15 062 (1995).